

## OPERATIONAL EFFECTIVENESS OF PHASE-CHRONOMETRIC AND NEURODIAGNOSTIC METHODS FOR CONTROLLING ROLLING-ELEMENT BEARING DEGRADATION

A. S. Komshin, K. G. Potapov,  
V. I. Pronyakin, and A. B. Syritskii

UDC 006.91:531.717:681.2.088

*In the present study, problems associated with monitoring the condition of rolling-element bearings (REBs) – one of the most common technical devices of rotor units in machines and mechanisms – are considered. A novel approach to metrological support and assessment of the technical condition of rolling-element bearings during operation is presented. Existing approaches are analyzed, including methods of vibration diagnostics, envelope analysis, wavelet analysis, and others. The application of the phase-chronometric and neurodiagnostic methods for monitoring a bearing over its life cycle is considered. For this purpose, a unified format of measurement information was used. The possibility of providing REB diagnostics on the basis of measurement information obtained from the shaft and the cage is evaluated.*

**Keywords:** *metrological support, measurement, degradation, rolling-element bearing, measuring technology, defect, mathematical model, phase-chronometric method, information efficiency, neurodiagnostics.*

**Introduction.** Currently, rolling-element bearings (REBs) are the most common technical devices for supporting the rotor units of a wide variety of machines and mechanisms. The reliability and performance of these units are largely determined by the bearings, which are generally considered to be their weakest links, thus requiring constant monitoring.

According to researchers, bearing failures may occur for several reasons. The most poorly-controlled defects involve those arising from the development of cracks and as a result of the impact of cyclic fatigue loads [1, 2]. The combination of these factors makes the service life of a bearing extremely unpredictable [3]. In [1], a diagram of a typical bearing failure is presented including the initiation stage of defect preceding bearing failure. In [4], the original kernel extreme learning machine (K-ELM) method, designed for analyzing the initial data of bearing vibration, is considered. The advantages of this method involve improved quality of training and the classification of measurement information about the functioning of the bearing for optimizing the various support vectors, i.e., key parameters of an improved K-ELM, as well as the application of a single-layer perceptron.

Among the most common methods and tools are vibration diagnostics of bearing elements with envelope analysis under nonstationary conditions [5–8]. Thus, in [7], the application of digital technologies and spectral analysis variations according to the envelope method are demonstrated for obtaining a significant effect when diagnosing individual bearing defects. However, only certain problems of bearing diagnostics at the life-cycle stages are solved by this approach.

Some studies in the field of bearing diagnostics are devoted not to the analysis of individual components of vibration along the axes, but rather to the mathematical analysis of the spatial acceleration vector in terms of a measuring signal for monitoring the condition of REBs. In the case of a faulty bearing, the study results illustrate a number of advantages in the analysis of the spatial vibration vector. An additional envelope analysis allows a higher accuracy of the load axis envelope spectrum to be obtained [9, 10]. Separately, an algorithmic approach based on the Holder coefficient and feature extraction within the framework of entropy theory is noted, along with intelligent recognition of bearing faults. Existing approaches are used for assessing the real time technical condition of an REB based on artificial intelligence [11].

Russian scientists have accumulated significant experience in solving problems associated with monitoring and diagnostics of bearings. Approaches to assessment of the technical condition of REBs include thermal diagnostics, vibration analysis, electrical conductivity, acoustic emission, and neural networks [12–19].

Each of the above-presented methods is aimed at solving many problems of bearing diagnostics and identifying individual defects, especially in lumped systems (on test benches, in conditions of access to the bearing and its elements, at high rotation velocities, etc.). However, at the present time, no comprehensive assessment and maintenance of bearings is available at all stages of the life cycle.

Depending on the sources of disturbance, the REB vibration spectrum of an electric machine is divided into several ranges. In the microwave range (500–20000 Hz), the use of demodulation methods for analyzing a vibroacoustic signal in the resonance frequency zone can reveal incipient defects at the earliest stages of development. In the high-frequency range (2000–20000 Hz), the stochastic acoustic model, which takes into account the modulation properties of forced oscillations of the mechanism nodes, is recommended for consideration. In the mid-frequency range (200–2000 Hz), it is necessary to construct a diagnostic model taking into account the quasi-polyharmonic parametric effect of oscillations and the nonlinear interaction of mechanism elements. This implies the beginning of the defect transfer from some bearing elements to others, i.e., the beginning of the bearing's destruction, as well as indicating its pre-failure state. In the low-frequency range (0–300 Hz), oscillations are mainly caused by the forces of unbalanced rotating masses; here, good results are provided by deterministic methods for identifying mechanical systems.

The classical approach, requiring the use of various methods and means of vibration and acoustic diagnostics to monitor various bearing defects at different stages of the life cycle, implies the solution of individual specific problems at each stage.

Thus, in order to obtain reliable measurement information about each stage of their operational life cycles, a unified approach to diagnostics and monitoring of bearings is required, including [20]:

- the development of test methods based on common scientific principles for all stages of the object's life cycle;
- the application of a minimum nomenclature of measured physical quantities;
- the creation of a unified methodological approach to assessing the current technical condition of REBs.

**Phase-chronometric method in the diagnostics of rotary machines and mechanisms.** The phase-chronometric (PCM) method was developed at the Bauman Moscow State Technical University. The development of this approach allowed the multisystem approach to REB diagnostics to be discarded in favor of a unified PCM system capable of providing effective information and metrological support of the bearing not only at the operation stage, but also throughout its entire life cycle [21–24]. In PCM diagnostics, time is the only measurable parameter. At all stages of diagnostics, the same problem is solved: variations in the time intervals of the bearing rotating elements are measured and projected according to the given algorithms onto an ideal sample (or model), then the measured and projected variations in the time intervals are compared followed by a diagnosis of the bearing condition at the time of measurement on the basis of the comparison results. At present, the sensitivity of PCM systems consists of a few nanoseconds. This is sufficient to cover the entire frequency range of vibration and vibroacoustic diagnostics indicated above, identify incipient defects of all bearing elements at the earliest stage including tracking their development throughout the entire period of operation, and give an early warning signal about the need to remove a degraded bearing from operation.

In contrast to vibration diagnostics approaches, PCM analysis and testing methods are based on uniform scientific principles for all stages of a bearing's life cycle. At the same time, the nomenclature of measured physical quantities is minimized with a unified methodological approach created for assessing the current technical state of REBs. Thus, all the achievements and innovations of the PCM method applied to other objects can be used to diagnose a particular bearing.

The first PCM bearing diagnostics systems were developed taking into account the possible placement of measuring sensors directly on the diagnosed elements: rings, rotation elements, and a cage. Figure 1 shows a diagram of the PCM diagnostics of a ball bearing. The multichannel diagnostic system consists of separator sensors, which generate electrical impulses when rolling elements pass  $\pi$  in front of the sensors, and elements (for example, rivets) of the separator. Reactive optical (laser), inductive or Hall sensors are used. The diagnostic device can also include a sensor for a rotating inner ring mounted on shaft 3 and a reference signal sensor 4. The reference signal corresponds to a complete revolution of the rotating inner ring and starts the total timer.

The impulses of the measuring sensors are sent to unit 5 (PCM adapter) for measuring the time intervals between impulses, where they are converted into measuring impulses. Then the time intervals are measured, encoded, and transmitted

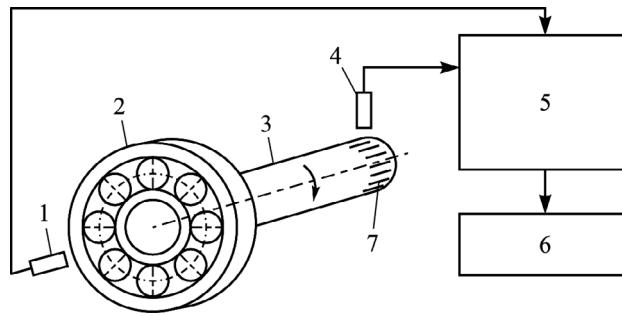


Fig. 1. PCM diagnostics scheme of a ball REB: 1) cage sensor; 2) ball REB; 3) shaft; 4) reference sensor; 5) block for measuring time intervals; 6) computer; 7) information labels.

to the block for generating and analyzing the series of time intervals. During the operation of the bearing, the analog signal of the sensor is converted into measuring impulses in the PCM adapter with subsequent transfer for analysis in the computer 6. When the bearing rotates, the time intervals corresponding to the angles of the shaft 3 and the cage rotation are recorded.

Let us consider a system consisting of an electric engine, a coupling, a shaft on two bearing supports, and a load. The power balance equation for systems with friction-caused energy losses can be written in the form

$$P_{in} = P_{out} + P_{fric},$$

where  $P_{in}$  is the input power;  $P_{out}$  is the output power;  $P_{fric}$  is the power losses due to friction.

Power can be calculated as the product of the force moment and the angular velocity of rotation. Then the balance equation for the system in Fig. 1 can be rewritten as

$$M_e \omega_e = M_{load} \omega_{shaft} + (M_{bear1} \omega_{shaft} + M_{bear2} \omega_{shaft}),$$

where  $M_e$ ,  $\omega_e$  are the moment of force and angular velocity of the engine, respectively;  $M_{load}$  is the shaft loading moment;  $\omega_{shaft}$  is the angular velocity of the shaft;  $M_{bear1,2}$  are the resistance moments of bearings 1, 2.

Assuming the engine to deliver constant power at a steady state of system operation, the following equilibrium equation is valid

$$(M_{load0} + M_{bear10} + M_{bear20}) \omega_0 = (M_{load1} + M_{bear11} + M_{bear21}) \omega_1, \quad (1)$$

where subscripts 0 and 1 denote the initial state of the system and the state registered at a given time interval, respectively.

Equation (1) can be rewritten in the PCM form:

$$(M_{load0} + M_{bear10} + M_{bear20}) 2\pi / (\tau_0 k) = (M_{load1} + M_{bear11} + M_{bear21}) 2\pi / (\tau_1 k), \quad (2)$$

where  $\tau_0$ ,  $\tau_1$  are the registered fractions of shaft revolution;  $k$  is the number of fractions into which the revolution is divided.

Various bearing defects affect the power balance, causing different changes in the angular velocity of rotation. Figure 2 illustrates the sliding process of rolling elements in the front spindle bearing of a metal-cutting machine at a spindle speed of 1000 rpm (where  $D$  is the variations in time intervals;  $n$  is the number of the phase quantum; segments shown in the upper part of the figure reflect the  $T_{slide}$  periods of passing the sliding time intervals of the rolling elements). In the absence of rolling element sliding, the character of rotation turns to be generally uniform without a large number of sharp jumps. When sliding occurs, sharp jumps in the time intervals appear on the shaft rotation chronogram. In accordance with the balance equation (2), a periodic increase in the resistance moment of the system occurs. The weakening of one support leads to a decrease in the rigidity of the system and the appearance of imbalance and concomitant forces of gyroscopic moment. As a result, the load on the second, more rigid, support increases, followed by its manifestation.

Additional information is provided from the spectral analysis of chronogram autocorrelation functions (ACF). The frequencies present in the ACF spectra are multiples of the frequency of the rolling elements along the inner ring. Figure 3 represents the ACF spectra with and without sliding.

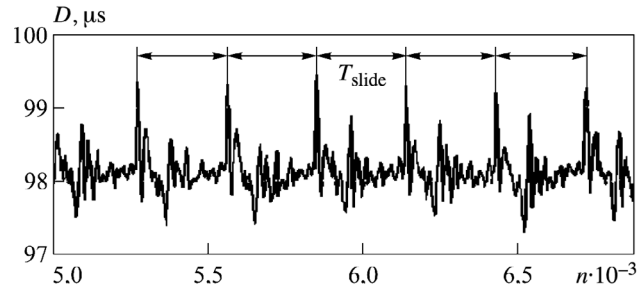


Fig. 2. Chronogram of bearing rotation: sliding of rolling elements of the bearing in idle mode.

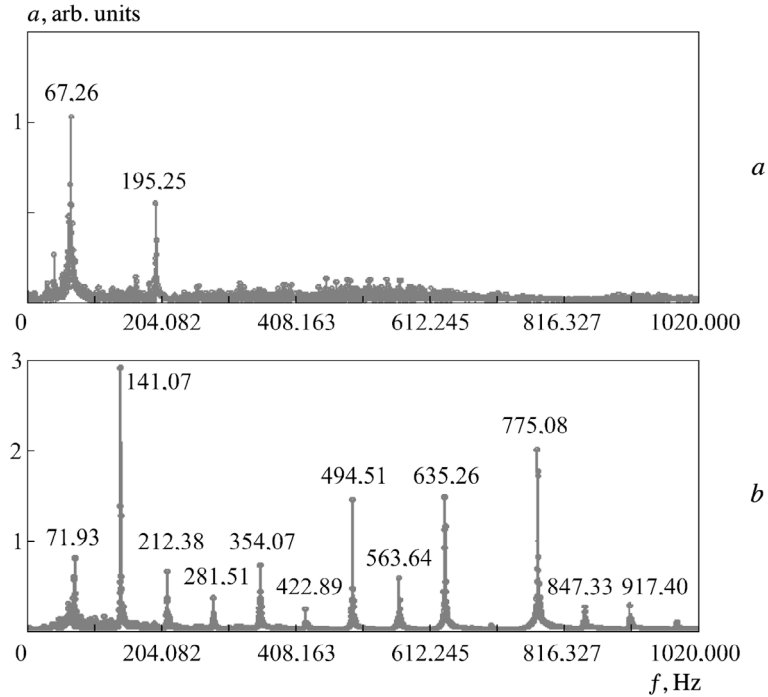


Fig. 3. Spectrum of autocorrelation functions with amplitude  $a$  in idle mode without ( $a$ ) and with sliding ( $b$ ).

Let us consider the following situation: suppose the rolling element defect – for example, chipping in a localized zone – has formed in one of the bearings of the above-described system. Then, when the rolling element passes this zone, a micro-shock occurs. From the perspective of the power balance equation, the micro-shock leads to an abrupt change in the bearing resistance moment, causing changes in the recorded time intervals. A jump in the force moment occurs when, in the process of making a revolution around its axis, the rolling element hits the path having a defective area. And since there are two paths (inner and outer rings), the number of jumps is doubled.

If the rotation is caused by the movement of the inner ring, the  $f_b$  rotation frequency of the element (ball) around its axis can be determined from the expression

$$f_b = f_{i,r} (d_{av}/d_b - 1),$$

where  $f_{i,r}$  is the rotation frequency of the inner ring;  $d_b, d_{av}$  are the diameters of the rolling elements and the average diameter of the bearing, respectively.

For implementation of the model experiment, let us assume the following parameter values:  $d_{av} = 85$  mm,  $d_b = 15$  mm,  $f_{i,r} = 1000$  rpm.

The system contains random noise associated with the nonlinearity of the gaps, distributed according to the normal law with zero expectation and standard deviation  $\sigma = 0.0004(625f_{i,r})^{-1}$  (one revolution is divided into 625 fractions).

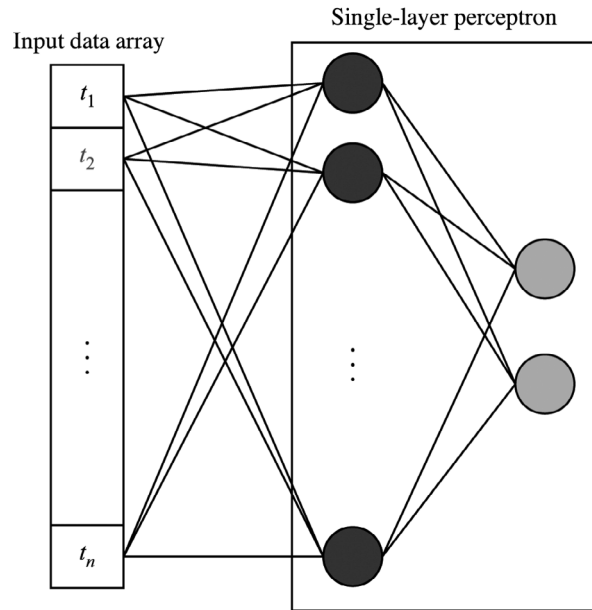


Fig. 4. Neural network diagram.

Under the given bearing parameters, the rolling element must make five revolutions around its axis in one revolution of the inner ring. However, taking into account two beats during one revolution, 10 peaks will be distinguished in the shaft rotation chronogram. The dominant frequency responsible for the disturbances in the rotation chronogram is obtained via spectral analysis.

Thus, with a rolling element defect in the shaft rotation chronogram, the observed distinct jumps can be attributed to a sharp change in the moment of resistance. At the same time, a frequency equal to the doubled rotation frequency of the element (ball or roller) around its axis will be allocated in the ACF spectrum.

**Application of a neural network for diagnosing bearing condition.** The demonstrated approach to diagnostics can additionally be developed using a neural network. Currently, neural networks are increasingly used in science, technology, medicine, trade, and other industries. Although the concept of neural networks first appeared in 1943 [30], with the first perceptron (cybernetic model of the brain) appearing in 1958 [31], half a century would pass before their general application due to the lack of the “big data” concept prior to the advent of the Internet. Following this revolution, neural networks turned out to be effective precisely in processing large amounts of information while unrevealing their potential in other cases.

In our study, a neural network was tasked with correct identification of the bearing defect. For these purposes, using the Keras [32] and TensorFlow [33] libraries of the Python programming language, a single-layer perceptron was developed with the diagram provided in Fig. 4, where  $t_{1,2,\dots,n}$  are the time intervals forming an array of input data.

*Perceptron configuration*

```

Model type . . . . . .sequential
Layer type . . . . . .fully connected
Layers . . . . . .input (625 neurons, reLU activation function),
                  output (2 neurons, softmax activation function)
Input data . . . . . .a data array with a dimension of 625 values
Metric . . . . . .accuracy
Error calculation method . . . . . .Adam
Loss function . . . . . .sparse cross-categorical entropy
Type of training . . . . . .by instruction

```

In this case, the use of the perceptron model is justified by the fact that such neural networks cope well with classification tasks. A continuous series of time intervals, divided into separate cycles, can be represented as a kind of individual

one-dimensional image for each state of the mechanism or its node. In this regard, this problem appears to be close to the problem of image identification.

It should be noted that the number of neurons in the input and output layers should not be chosen randomly. Since the input data array has 625 elements, it is logical to use the same number of neurons in the input layer. Since the current task involves the determination of the bare fact of a defect without classifying it, the output layer has only two neurons: 0 (no defect) and 1 (defect). The input data for the neural network are prepared as follows:

- arrays of initial data are divided into cycles, each having 625 values;
- each cycle inside the arrays of “normal” and “defective” values is labeled “0” and “1,” respectively;
- arrays are combined and mixed (for better neural network training);
- the mixed single array is divided into training and test arrays in the ratio of 66:33.

The training of the perceptron was performed at 50 epochs, while the values of the weights providing the highest accuracy were saved to a file. As a result of calculations performed by the neural network, the probability of correct identification on the training and test data was 98 and 95%, respectively.

It should be noted that no operation of the neural network under real conditions was implemented: the training was performed on data processed according to the above-proposed method, i.e., with a known end result (whether there is sliding or not). Here it was important to demonstrate the potential of using neural networks in technical diagnostics. Having trained the neural network on the data generated by this model, it is possible to effectively use the network with the available verified mathematical model in real diagnostic situations involving a wide range of potential defects.

One of the key parameters in obtaining information corresponding to a measurement result comprises the useful component of measurement information. In 1948, in terms of a measure for the amount of information, the American engineer and mathematician C. Shannon introduced the concept of entropy [34] expressing uncertainty. Later P. V. Novitskii proposed to apply information theory to measuring instruments [35]. Here, the amount of information is defined as the difference in entropies before  $H(x)$  and after  $H(x/x_{\text{meas}})$  measurements [36]:

$$I = H(x) - H(x/x_{\text{meas}}).$$

The entropy of a discrete source is calculated by the formula [34]:

$$H(x) = -\sum_i p(x_i) \log_2 p(x_i), \quad (3)$$

where  $p_i$  is the probability of  $i$ th event.

For a continuous source, Eq. (3) is transformed to the form [34, 36]:

$$H(x) = -\int_{-\infty}^{+\infty} p(x) \log_2 p(x) dx.$$

When measuring a random value on the  $[x_1; x_2]$  interval with an  $\Delta$  error for uniformly distributed values, the expression [36] is valid:

$$I = \log_2[(x_2 - x_1)/(2\Delta)] = \log_2 N. \quad (4)$$

Equality (4) is also valid for any other random values distribution laws, provided that the measurement uncertainty interval is determined from the entropy [36]. In order to assess the information capacity of the PCM method, the  $N$  value should be understood as the ratio of the  $T$  single time interval and the  $2\Delta t$  entropic measurement uncertainty. At present, the limiting error of measuring the  $\Delta t$  time intervals in the PCM method by the existing technical means comprises 50 ns [26].

The information capacity of the PCM method was calculated using Eq. (4):

$$I = \log_2(2^{-1} \cdot 5^{-1} \cdot 10^8) = 23.3 \text{ bits.}$$

The information capacity of the vibration diagnostics method can be estimated in a similar way. As a result of reviewing the catalogs of modern vibration sensors from different companies, the maximum value of the vibration acceleration measurement error was not more than  $10 \mu\text{m/s}^2$ . In accordance with the formula (4), the information capacity of the vibration diagnostics method was calculated:

$$I = \log_2(2^{-1} \cdot 10^5) = 15.6 \text{ bits.}$$

Thus, the PCM method provides more information, since at present no quantity is measured more accurately than time intervals [26].

**Conclusion.** Diagnostics of REBs using the proposed PCM method covers the entire frequency range of vibration and acoustic diagnostics to identify incipient defects of REB elements at the earliest stage. In this case, it is possible to track the development of defects throughout the entire REB operational period and proactively require the removal of the degrading item from operation. The application of a neural network in the diagnostics of REBs has great potential, allowing the identification of defects with a high (95%) degree of reliability. According to the calculations of the metrological characteristics of the measuring channel, the error in transmitting the information signal via fiber-optic communication lines is  $\pm 5 \cdot 10^{-9}$  s. Estimates of the information capacity calculated for the PCM method and vibration diagnostics are 23 and 15 bits, respectively. Thus, the high accuracy of determining the time intervals provides the possibility of further increasing the information capacity of the PCM method.

The present study was supported by a grant from the President of the Russian Federation for state support of young Russian scientists – Doctors of Science (MD-1209.2020.8).

The results of the study were partially obtained using the equipment of the Center for Collective Use of High-Precision Measuring Technologies in Photonics (ckp.vniiofi.ru), created on the basis of the All-Russia Research Institute of Optophysical Measurements (VNIIOFI).

## REFERENCES

1. A. Kumar and R. Kumar, *J Nondestruct Eval*, **38**, 5 (2019), <https://doi.org/10.1007/s10921-018-0543-8>.
2. J. Dybata and R. Zimroz, *Appl Acoust*, **77**, 195–203 (2014), DOI:10.1016/j.apacoust.2013.09.001.
3. N.G. Nikolaou and I.A. Antoniadis, *NDT & E Int.*, **35**, 197–205 (2002), <https://doi.org/10.1016/j.apacoust.2013.09.001>.
4. L. Zheng, Y. Xiang, and C. Sheng, *J. Braz. Soc. Mech. Sci. Eng.*, **41**, 505 (2019), <https://doi.org/10.1007/s40430-019-2011-5>.
5. M. D. Prieto, G. Cirrincione, and A. G. Espinosa, *IEEE Trans. Industr. Electr.*, **8**, 3398–3407 (2013), <https://doi.org/10.1109/TIE.2012.2219838>.
6. I. Attoui, B. Oudjani, N. Boutasseta, et al., *Int. J. Adv. Manuf. Tech.*, **106**, 3409–3435 (2020), <https://doi.org/10.1007/s00170-019-04729-4>.
7. R. B. Randall and J., *Antoni, Mech. Syst. Signal Pr.*, **25**, No. 2, 485–520 (2011), <https://doi.org/10.1016/j.ymssp.2010.07.017>.
8. S. Chatterton, P. Pennacchi, A. Vania, and P. Borghesani, *Proc. 9th IFToMM Int. Conf. Rotor Dynamics. Mechanisms and Machine Science*, Springer, Cham (2015), Vol. 21.
9. M. Cotogno, M. Coconcelli, and R. Rubini, *Advances in Condition Monitoring of Machinery in Non-Stationary Operations. Lecture Notes in Mechanical Engineering*, Springer, Berlin, Heidelberg (2014).
10. P. Borghesani, R. Ricci, S. Chatterton, and P. Pennacchi, *Advances in Condition Monitoring of Machinery in Non-Stationary Operations. Lecture Notes in Mechanical Engineering*, Springer, Berlin, Heidelberg (2014).
11. Y. Ying, J. Li, J. Li, and Z. Chen, *Advanced Hybrid Information Processing. ADHIP 2017. Lecture Notes of the Institute for Computer Sciences, Social Informatics and Telecommunications Engineering*, Springer, Cham (2018), Vol. 219.
12. R. S. Tikhonov and N. P. Starostin, “Thermal diagnostics of friction in a sliding bearing system taking into account shaft rotation,” *Mekh., Resurs Diagn. Mater. Konstr.*, 83–83 (2016).
13. S. V. Korotkevich, O. V. Kholodilov, V. V. Kravchenko, et al., “Incoming inspection of rolling-element bearings by physical methods,” *Remont. Vosstan. Moderniz.*, No. 11, 24–31 (2015).
14. V. V. Mishin and A. S. Pashmentova, “A device for diagnosing a rolling-element bearing during incoming inspection,” *Sovr. Mater., Tekhn. Tekhnol.*, No. 1 (9), (2017).
15. M. P. Kozochkin, F. S. Sabirov, A. N. Bogan, and K. V. Myslivtsev, “Diagnostics of rolling-element bearings during machine operation based on vibration signal analysis,” *Stanki Instr.*, No. 1, 21–25 (2013).

16. V. V. Yurkevich and P. V. Lushnikov, "Diagnostics of rolling-element bearings," *Stanki Instr.*, No. 1, 97–99 (2015).
17. E. A. Kudryavtsev, "Possible ways of using phase timing for diagnostics of rolling stock," *Zheleznodor. Transp.*, No. 12, 51–53 (2015).
18. E. A. Kudryavtsev, "Assessment of the technical condition of axle-box rolling-element bearings for railroad cars," *Remont. Vosstan. Moderniz.*, No. 6, 26–31 (2013).
19. M. P. Kozochkin and F. S. Sabirov, "Measurement of spatial vibrations for diagnostics of the assembly quality of spindle assemblies," *Izmer. Tekhn.*, No. 12, 49–52 (2016).
20. V. I. Pronyakin, E. A. Kudryavtsev, A. S. Komshin, and K. G. Potapov, "Diagnostics of rolling-element bearings by phase-chronometric method," *Izv. Vyssh. Uchebn. Zaved. Mashinostr.*, No. 3 (684), (2017).
21. E. A. Kudryavtsev, A. S. Komshin, K. G. Potapov, and V. I. Pronyakin, "A new concept of PCM diagnostics of rolling-element bearings," *Remont. Vosstan. Moderniz.*, No. 4, 18–24 (2017).
22. M. I. Kiselev, A. S. Komshin, and A. B. Syritskii, "Prediction of the technical state of a turning tool based on phase-chronometric measuring information," *Izmer. Tekhn.*, No. 11, 8–11 (2017), <https://doi.org/10.32446/0368-1025it.2017-11-8-11>.
23. A. S. Komshin, "Mathematical modeling of measuring and computational control of electromechanical parameters of turbine units by phase-chronometric method," *Izmer. Tekhn.*, No. 8, 12–15 (2013).
24. A. B. Syritskii, "Measuring the wear of a cutting tool by the phase-chronometric method during processing," *Izmer. Tekhn.*, No. 6, 30–32 (2016).
25. A. S. Komshin and C. R. Orlova, "Control of degradation of structural materials during operation on the example of string elements," *Izmer. Tekhn.*, No. 6, 26–29 (2016).
26. M. I. Kiselev, V. I. Pronyakin, and A. K. Tulekbaeva, *IOP Conf. Ser.: Mater. Sci. Eng.*, **312**, No. 1, 012012 (2018), <https://doi.org/10.1088/1757-899X/312/1/012012>.
27. A. I. Leontiev and S. A. Burtsev, *Dokl. Physics*, **61**, No. 11, 543–545 (2016), <https://doi.org/10.1134/S1028335816110100>.
28. R. A. Poshekhonov, G. A. Arutyunyan, S. A. Pankratov, et al., *Semiconductors*, **51**, No. 8, 981–985 (2017), <https://doi.org/10.1134/S1063782617080255>.
29. V. Lavrinenko, A. Polyakova, and A. Polyakov, *MATEC Web Conf.*, **224**, 02074 (2018), <https://doi.org/10.1051/mateconf/201822402074>.
30. N. Wiener. *Cybernetics. Ch. I* [Russian translation], Sov. Radio, Moscow (1961), 2nd ed.
31. Yu. F. Golubev, *Neural Network Methods in Mechatronics*, Izd. MGU im. Lomonosova, Moscow (2007).
32. *Keras: The Python Deep Learning Library*, [www.keras.io/](http://www.keras.io/), acc. 02/20/2020.
33. *TensorFlow: An End-to-End Open Source Machine Learning Platform*, [www.tensorflow.org](http://www.tensorflow.org/), acc. 02/20/2020.
34. M. Kraus and E. Voshni, *Measuring Information Systems* [Russian translation], Mir, Moscow (1975).
35. P. V. Novitskii and I. A. Zograf, *Estimation of Measurement Results Errors*, Energoatomizdat, Leningrad (1991), 2nd ed.
36. S. V. Slepova, *Basics of Accuracy of Measuring Devices: Teach. Aid*, Izd. YuUrGU, Chelyabinsk (2008).